Experimental study of mass transfer by volatilization inside a portable wind tunnel used to estimate emission rates for odorous compounds

Estudo experimental de transferência de massa por volatilização no interior de um túnel de vento portátil utilizado para estimativa das taxas de emissão para compostos odorantes

Philipe Uhlig Siqueira[1] (iD), Laize Nalli de Freitas[2] (iD), Matheus de Araújo Siqueira[2] (iD), Pâmela Rossoni Lima[2] (iD), Jane Meri Santos[2] (iD), Bruno Furieri[2] (iD)

ABSTRACT

Wastewater treatment plants are sources of hydrogen sulfide in urban environments. This compound, at certain concentrations, may be associated with compromising the health and well-being of populations living near such sources, characterized by diffuse emission, which makes it difficult to quantify. The portable wind tunnel is one of the devices used to measure this type of emission; however, this equipment is not capable of simulating all significant mass transport phenomena. Thus, this study investigated mass transfer at the liquid-gas interface of hydrogen sulfide by estimating the global mass transfer coefficient within the portable wind tunnel. The inlet flow rate into the system ranged from 600 to 1,800 L min^{-1}, and the analysis of concentration decay in the liquid phase was performed using spectrophotometry. The observed exponential decay is consistent with the adopted hypotheses; however, no significant variation in the mass transfer coefficient was observed for different system operation flow rates. The average value found was $2.70\times10^{-5}\pm2.99\times10^{-6}$ m s^{-1}. In summary, this study contributed to understanding the mass transfer of hydrogen sulfide in wastewater treatment environments using a portable wind tunnel as an experimental tool.

Keywords: hydrogen sulfide; volatilization; portable wind tunnel; odor; mass transfer coefficient.

RESUMO

Estações de tratamento de esgoto são fontes de sulfeto de hidrogênio em ambientes urbanos. Este composto, em determinadas concentrações, pode estar associado ao comprometimento da saúde e bem-estar das populações que residem próximas a tais fontes, caracterizadas por sua emissão difusa, o que dificulta sua quantificação. O túnel de vento portátil é um dos dispositivos aplicados na mensuração deste tipo de emissão, porém, este equipamento não é capaz de simular todos os fenômenos significativos para o transporte de massa. Desta forma, este estudo investigou a transferência de massa na interface líquido-gás do sulfeto de hidrogênio, estimando o coeficiente global de transferência de massa no interior do túnel de vento portátil. A vazão de entrada no sistema variou entre 600 e 1.800 L min^{-1} e a análise do decaimento da concentração na fase líquida foi realizada por espectrofotometria. O decaimento exponencial observado é condizente com as hipóteses adotadas, entretanto, nenhuma variação significativa no coeficiente de transferência de massa foi observada para diferentes vazões de operação do sistema. O valor médio encontrado foi de $2,70\times10^{-5}\pm2,99\times10^{-6}$ m s^{-1}. Em resumo, o presente estudo contribuiu para a compreensão da transferência de massa do sulfeto de hidrogênio em ambientes de tratamento de efluentes, utilizando um túnel de vento portátil como ferramenta experimental.

Palavras-chave: sulfeto de hidrogênio; volatilização; túnel de vento portátil; odor; coeficiente de transferência de massa.

[1]Pontifícia Universidade Católica do Rio de Janeiro – Rio de Janeiro (RJ), Brazil.

[2]Universidade Federal do Espírito Santo – Rio de Janeiro (RJ), Brazil.

Correspondence address: Philipe Uhlig Siqueira – Pontifícia Universidade Católica do Rio de Janeiro (PUC-Rio) – Rua Marquês de São Vicente, 225 – Gávea – CEP: 22451-900 – Rio de Janeiro (RJ), Brazil. E-mail: philipe.uhlig@gmail.com

Introduction

Odor is a response perceived through the reaction to a chemical stimulus in the human olfactory system. Although it is not necessarily associated with toxic or harmful effects on human health, it does cause discomfort to well-being.

A potential source of odor emissions in urbanized areas is wastewater treatment plants (Teixeira et al., 2018) due to the emission of odorous compounds with low perception thresholds, including sulfur, nitrogen, and volatile organic compounds (VOCs), such as hydrogen sulfide (H_2S), methanethiol, ammonia and methylamine (Jiang et al., 2017; Vitko et al., 2022). Passive surfaces such as treatment ponds are common in these plants and are characterized by the fact that there is no forced gas flow within the liquid phase.

Among the various compounds emitted, H_2S is commonly related to odor emissions in wastewater treatment plants. In addition, this compound has been used as an indicator for odor emissions in wastewater treatment plants due to its low odor perception threshold and because it is easy to monitor, as there are specific sensors for this gas. Consequently, H_2S levels can be continuously monitored (Suffet and Braithwaite, 2019; Vitko et al., 2022).

Determining the emission rate of odorous compounds is an important aspect of truly understanding the environmental impacts and health effects on populations exposed to the aforementioned sources. There are three methods for estimating the odor emission rate: 1. Use of empirical or theoretical models based on the physics of mass transfer (Deacon, 1977; Mackay and Yeun, 1983; Gostelow et al., 2001; Prata et al., 2018b), 2. Application of indirect methods with the aid of meteorological measurements (Tran et al., 2018) and 3. Direct method, using enclosing equipment over a part of the emitting source (Guillot et al., 2014; Prata et al., 2018b).

The use of indirect techniques is costly due to the large number of samples or measurements to be taken (Hudson and Ayoko, 2008b; Capelli et al., 2013), as well as the need for simultaneous monitoring of meteorological conditions. Empirical and theoretical models are determined through laboratory experiments and simplifying assumptions applied to the physical principles of mass transfer, and the equations are only applicable to the conditions in which these assumptions are real (Prata et al., 2018b). Due to these limitations, direct methods have been widely studied to determine the emission rate of odorous compounds on passive surfaces (Prata et al., 2014, 2016, 2018a; Andreão et al., 2019; Lucernoni et al., 2017).

The portable wind tunnel (PWT) is one of the enclosing devices used in the direct method and, according to Hudson et al. (2008a), due to the relationship between wind speed and emission rates presented in the study, the wind tunnel has the potential to better simulate natural emission processes compared to other direct methods. However, research conducted using the PWT indicates that this device cannot represent all the factors relevant to the emission process (Liu et al., 2022). Therefore, studies are needed to understand the flow and mass transfer inside these devices, and one way to understand the behavior of enclosing devices is by quantifying mass transfer under controlled conditions.

Laboratory mass transfer studies for compounds dominated by gas and liquid phases have been conducted using a dynamic flux chamber (Prata et al., 2018a). However, for PWT, the literature points to experiments conducted only for compounds dominated by the gas phase or analyses conducted by the gas phase (Liu et al., 2015; Lucernoni et al., 2017), and there are no studies that quantify mass transport for compounds dominated by the liquid phase in a controlled environment.

Knowledge of the PWT behavior is of paramount importance in environmental engineering since the development of this device can be used to quantify the emission of useful odor to develop standards that establish the limit amount of odor emission of a given passive surface that mitigates the impact on populations near emitting sources. The use of PWT as a device for monitoring emissions from passive liquid sources reduces three types of problems: social, such as the population's dissatisfaction with local development; economic, such as the devaluation of real estate due to odor; and environmental, related to the emission of odorous compounds into the atmosphere.

In light of this, understanding that H_2S is a compound commonly emitted in wastewater treatment plants and normally used as an indicator for odor quantification due to its low perception threshold, and given that mass transfer has been investigated within the PWT, this study aims to carry out laboratory mass transfer experiments for H_2S using spectrophotometry in the liquid phase, in order to broaden the understanding of the device's behavior.

Methodology

Configuration of the experimental apparatus

Figure 1 shows a schematic diagram of the entire system comprising the wind tunnel, showing, from left to right, the frequency inverter, the fan, the activated carbon filter, the vortex flow meter, and the PWT. The latter consists of the flow development pipe, expansion zone, test section, contraction zone, and sampling zone. The experiments were conducted using the PWT of Wang et al. (2001), which differs from the tunnel developed by Jiang et al. (1995) by the extension and curvature of the gas phase sampling region, promoting better mixing of the compounds emitted by the passive surface with the reference gas inserted into the tunnel. The PWT was made of acrylic and its main section was 250 mm high, 800 mm long, and 400 mm wide.

The air supply to the interior of the equipment was provided by a centrifugal exhaust fan coupled to a three-phase motor (WEG W22, 2 HP, 3500 RPM). A frequency inverter (WEG CFW 300) was installed to control the fan rotation and allow tests using different inlet flow rates. An activated carbon filter was used to ensure a clean air supply for the system. The entire system was interconnected by corrugated pipes, and during the experiments, the wind tunnel was positioned over a 5 cm deep reservoir, where the ends of the reservoir fitted into the ends of the lower section of the test zone.
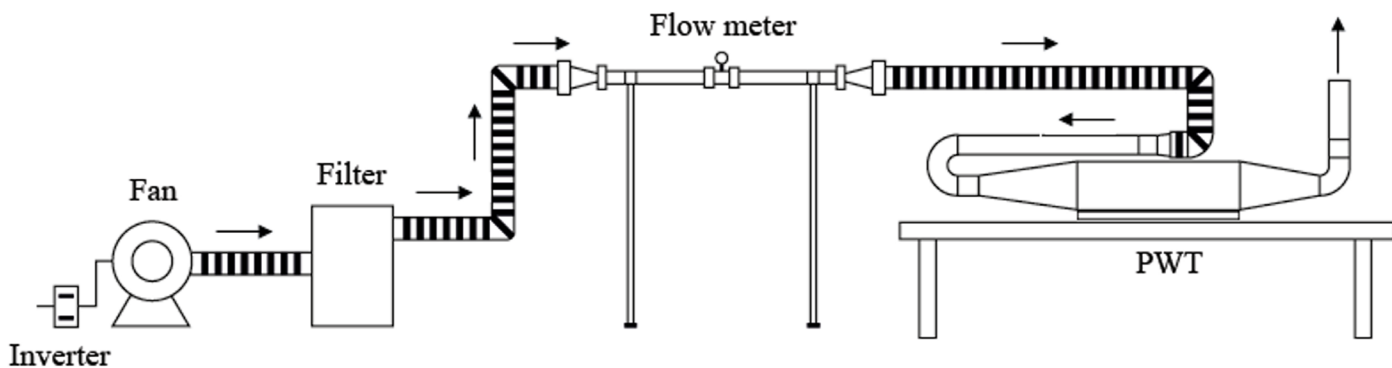
Figure 1 – Schematic diagram of the portable wind tunnel.

During the experiments, the system was inflated so that the gas mixture was released directly into the atmosphere, following operating parameters close to those expected in the field.

Measurement of flow conditions inside the apparatus

A thermometer (Soma 025) was used to measure the temperature of the liquid phase, and a thermohygrometer (Minipa MT-241) was installed at the beginning of the sampling section to measure the temperature and humidity of the gas phase. In addition, a thermohygrometer (Minipa MTH-1300) was positioned externally near the PWT to measure the temperature and humidity of the laboratory. A vortex flow meter (Yokogawa DY050-JBLAA1-2D/SCT) was used to monitor the flow in the system. The chosen carrier gas was atmospheric air.

Determination of the mass transfer coefficient

The two-film theory, proposed by Whitman in 1923, indicates that the mass flow at a liquid-gas interface can be calculated using Equations 1 and 2.

$$J = K_L \left(C_L - \frac{C_G}{K_H} \right) \tag{1}$$

$$\frac{1}{K_L} = \frac{1}{k_L} + \frac{1}{K_H k_G} \tag{2}$$

It can be seen that the flux (J) is the transport of mass through the interface area and, by rewriting Equation 1 as a function of the rate of mass change of the compound, Equation 3 is obtained (Arogo et al., 1999), as follows:

$$\frac{dM}{dt} = K_L A_{base} \left(C_L - \frac{C_G}{K_H} \right) \tag{3}$$

Where:

M = mass of the compound (kg);

K_L = global mass transfer coefficient (m s^{-1});

A_{base} = emitting area enclosed by the equipment (m²);

C_L and C_G = liquid and gas phase concentrations (Kg m^{-3}), respectively;

K_H = Henry's dimensionless coefficient; and

t = time

Since the experiments were conducted in the liquid phase, the variation in the mass of the compound over time implies the variation in the compound concentration in the liquid phase. Therefore, Equation 3 can be rewritten in terms of compound concentration of interest in the liquid phase, and Equation 4 is obtained.

$$\frac{dC_L}{dt} = -K_L \frac{A_{base}}{V} \left(C_L - \frac{C_G}{K_H} \right) \tag{4}$$

Once the carrier gas is filtered through an activated carbon system before reaching the liquid interface, it is understood that the concentration value in the gas phase will be much lower than it is in the liquid phase, making it possible to cancel out the C_G. Thus, Equation 4 was developed leading to Equations 5 and 6 by applying the limits of integration for concentrations, considering initial concentration in the liquid phase (C_0) and final concentration in the liquid phase after a certain time (C_L (t)), in which time varies from t_0 =0 to t.

$$\ln \left(\frac{C_L(t)}{C_0} \right) = -K_L \frac{A_{base}}{V} t \tag{5}$$

$$C_L(t) = C_0 e^{-K_L \frac{A_{base}}{V} t} \tag{6}$$

Equation 6 represents the decay of the concentration in the liquid phase, in which the exponential coefficient refers to the speed at which the decay occurs. Therefore, knowing all the variables in the equation, it is possible to determine the K_L by fitting an exponential profile curve to the periodic measurements taken in each experiment.

Thus, ultraviolet-visible (UV-VIS) spectrophotometry was used to determine the concentration of the compound. In order to ensure that the measured absorbance is only the result of wavelength interactions with the substance, a zero-concentration cuvette (blank) using the same solvent (deionized water) is used as a reference. Consequently, all measurements were compared with the blank before they were actually measured.

To analyze H_2S, according to Arogo et al. (1999), when this compound is diluted in an aqueous solution, it dissociates into three ions present in the solution, namely H^+ (hydrogen), HS^- (hydrogen; sulfur), and S^-_2 (sulfur). However, the mass fractions of these ions vary according to the pH of the aqueous solution. Unlike the ions present in the solution, only H_2S can be emitted into the atmosphere, so it is necessary to ensure that only H_2S is present in this solution. Therefore, by keeping the pH<5, only H_2S will be present in the aqueous solution. The literature shows that spectrophotometry measures this compound by measuring the HS^- ion. Thus, if it is kept at a pH between 10 and 14, only the HS^- ion will exist in the aqueous solution (Arogo et al., 1999). Considering that the pH of the aqueous solution was maintained at approximately 4 during the experiment, it is possible to state that the total sulfur concentration is equal to that of H_2S in the liquid phase.

Experimental procedure

H_2S is a compound dominated by the liquid phase, since its K_H has a value of 3.64 x 10^{-1} at a temperature of 20°C in the literature. This characteristic implies that the properties of the liquid phase influence the transfer of the compound more significantly than the gas phase. Thus, monitoring the liquid solution is extremely important to understand the mass transfer of this odorant compound.

Spectrophotometry at a wavelength of 231 nm was used for H_2S (Pouly et al., 1999; Santos et al., 2012). However, H_2S is not found naturally in the liquid phase, and chemical reactions are required to form this compound in the aqueous phase. H_2S (M≈34.08 g mol^{-1}) is formed by mixing sodium sulfide (Na_2S, M≈78.05 g mol^{-1}) with water (H_2O) according to the chemical reaction described below. However, for the calibration and subsequent experiment, Sigma-Aldrich sodium sulfide nonohydrate ($Na_2S \cdot 9H_2O$, M=240.18 g mol^{-1}) was used, which has a different molar mass and consequently changes the amount of mass to be used to generate the same concentration of H_2S.

$$Na_2S + 2 H_2O \leftrightarrow H_2S + 2 NaOH$$
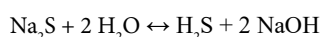
As the initial concentration of the experiment would be 5 mg L^{-1}, the calibration for the measurement with the spectrophotometer was conducted with six known concentrations, ranging from 1.0 to 6.0 mg L^{-1} varying by 1.0 mg L^{-1} among solutions. Therefore, a mother solution with a concentration of 1,000 mg L^{-1} was created and each reference solution was generated from it. It is worth noting that each solution obtained by diluting the mother solution was made just before the measurement, in order to reduce the effects of compound degradation.

Before the measurements with H_2S, two drops of a sodium hydroxide solution were inserted to ensure that only all the sulfide measured came from the ion HS^- (pH≈11). Such alkalinization is necessary because the 231 nm wavelength is capable of quantifying HS^- (Pouly et al., 1999; Santos et al., 2012) present in the solution. According to Arogo

et al. (1999) the aqueous solution pH indicates the fraction of sulfur compounds in it, and for pH≈10 the solution contains only HS^- as a sulfur compound.

The laboratory was previously prepared for the experiment. The spectrophotometer was switched on first, as it needs at least 15 minutes to start up, as indicated in the equipment manual. Then the balance was also switched on, with a waiting time of 30 minutes before weighing the Na_2S. The same reaction used to calibrate the spectrophotometer was used to generate 16.3 L (reservoir volume) at a concentration of 5 mg L^{-1}.

According to Arogo et al. (1999) the H_2S solution can dissociate into HS^- e S^{2-} depending on the pH of the aqueous solution. Therefore, the solution was acidified with sulfuric acid (H_2SO_4) while maintaining pH=4, measured with reactive strips, so that only H_2S is present in the tank. However, before each measurement, a drop of a 0.3 mol L^{-1} solution of NaOH was added to the cuvette to increase the pH to a range above 10.0 (pH≈11), also measured with reactive strips, so that only the HS^- ions remained in the sample. This procedure was adopted because the HS^- ion responds satisfactorily to the 231 nm wavelength. Consequently, measurements were made based on the concentration of HS^-.

Three tests were conducted for the H_2S at three different flow rates: 600, 1,200 and 1,800 L min^{-1}, giving average velocities in the inlet pipe of respectively 1.27, 2.55, and 3.82 m s^{-1}; and average velocities of 0.1, 0.2, and 0.3 m s^{-1} in the PWT test section, respectively. For each test, an initial measurement of the H_2S concentration in the liquid phase conducted out with the entire system assembled, but without the fan starting up. After the fan was started by means of the frequency inverter, a 10-minute stabilization period was adopted before measurements, which were taken approximately every 25 minutes, considering the time of the measurement of the first point as a reference. The 10-minute stabilization time was adopted as 75-fold the value of the characteristic time obtained by the ratio between the volume of the main section and the lowest flow rate applied. To collect the samples, a 4 mL volumetric pipette was used, with a diameter capable of passing through the holes in the tunnel and sufficient length to collect the samples close to the liquid-gas interface. Samples were taken by pipetting the liquid close to the surface layer and adding it to the cuvette after it had been prepared by double rinsing with the solution sampled at the time. Sampling was conducted in sequence from point 1 to point 6, where two samples were taken at each point in each series.

Results and Discussion

Mass transfer coefficients

As explained in the Method section, tests were conducted with three different flow rates (600; 1,200; and 1,800 L min^{-1}) and, for each test or flow rate, three repetitions were conducted on three consecutive

days, one test each day. Six points were sampled in each test and for each repetition. The relative humidity inside the apparatus averaged 49.6%, with a maximum of 55.0% and a minimum of 47.0%. The temperature values were analyzed separately. The temperature of the liquid phase averaged 20.5°C, with a maximum of 25.3°C and a minimum of 17.4°C, while the temperature inside the tunnel averaged 22.5°C, with a maximum of 26.2°C and a minimum of 20.0°C.

Curve fitting presentation

Figure 2 shows the concentration decay, dimensionless by the initial concentration of each test conducted. It is worth noting that two measurements were taken before the fan was started and they differ from each other. The first measurement was taken as the reference for dimensionless, resulting in different values of 1.0 on the ordinate of each graph.
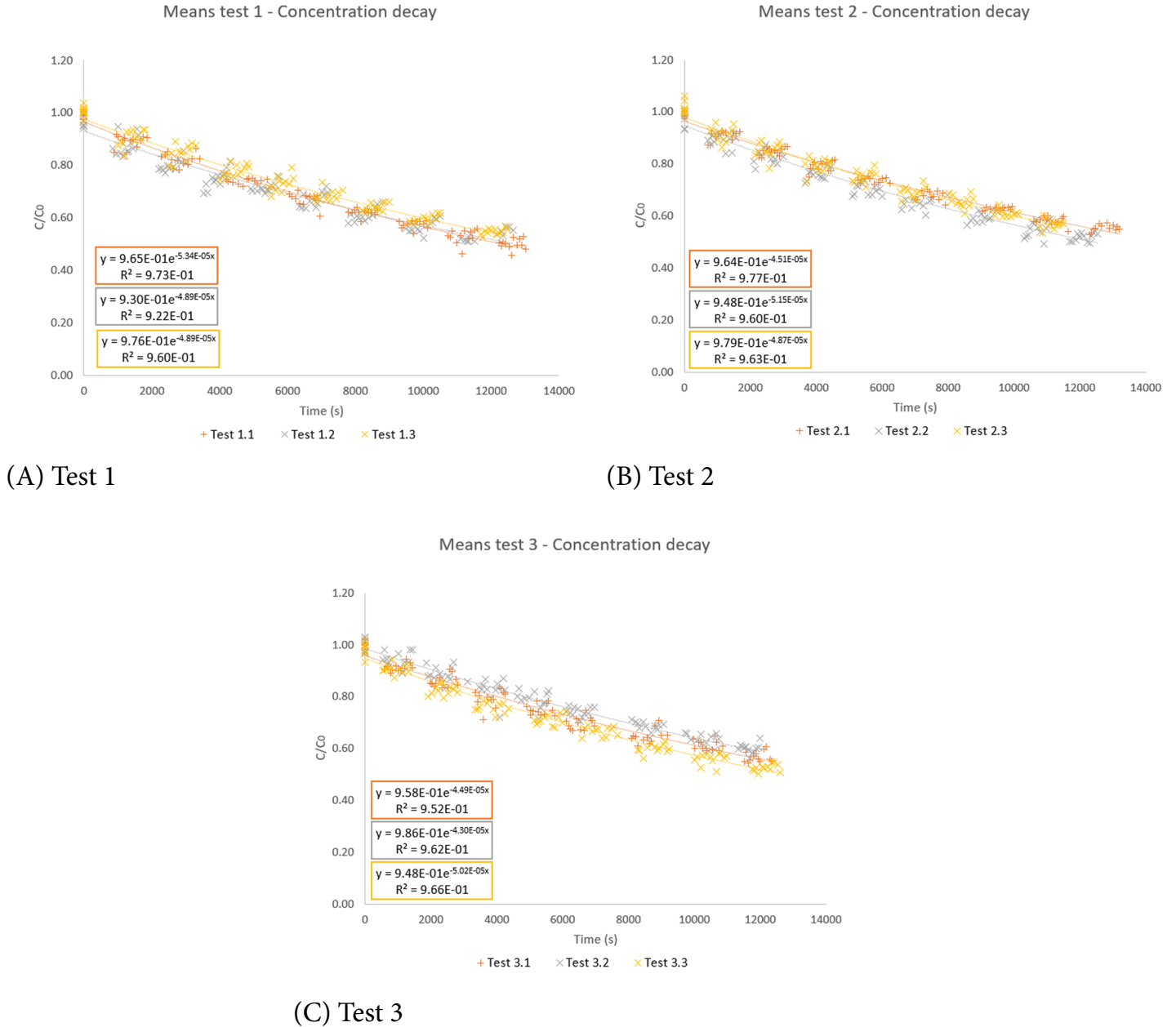

(A) Test 1

(B) Test 2

(C) Test 3

Figure 2 – Exponential adjustment for the mean of all points to obtain the global mass transfer coefficient.
y: fitting equation; R^2: coefficient of determination.

It can be seen that the exponential fitting was satisfactorily adapted to the decay of the compound concentration in the liquid phase, where the coefficients of determination (R^2) varied between 0.922 and 0.977 which, in an initial analysis, allow the K_L values to be determined using the methodology described, as the adjustment fits Equation 6.

By applying the natural logarithm to the expression obtained with the exponential fit (Equation 6), it is possible to carry out the linear fit (Equation 5), where the angular coefficient of the line is the value of K_L.

multiplied by the ratio of the surface area and the volume of the liquid solution. It is worth noting that, as described in Equation 5, an equation in the form of y=ax is expected, in which $y=\left(\frac{C_L(t)}{C_0}\right)\left(\frac{V}{A}\right)$ and $a=K_L$. For this reason, during the post-processing of the data, an adjustment was applied to the equations obtained, in which the intersections were forced to coincide at the origin. This adjustment brought the adjusted equations into line with the equations deduced from the hypotheses adopted. These graphs and adjustments are shown in Figure 3.
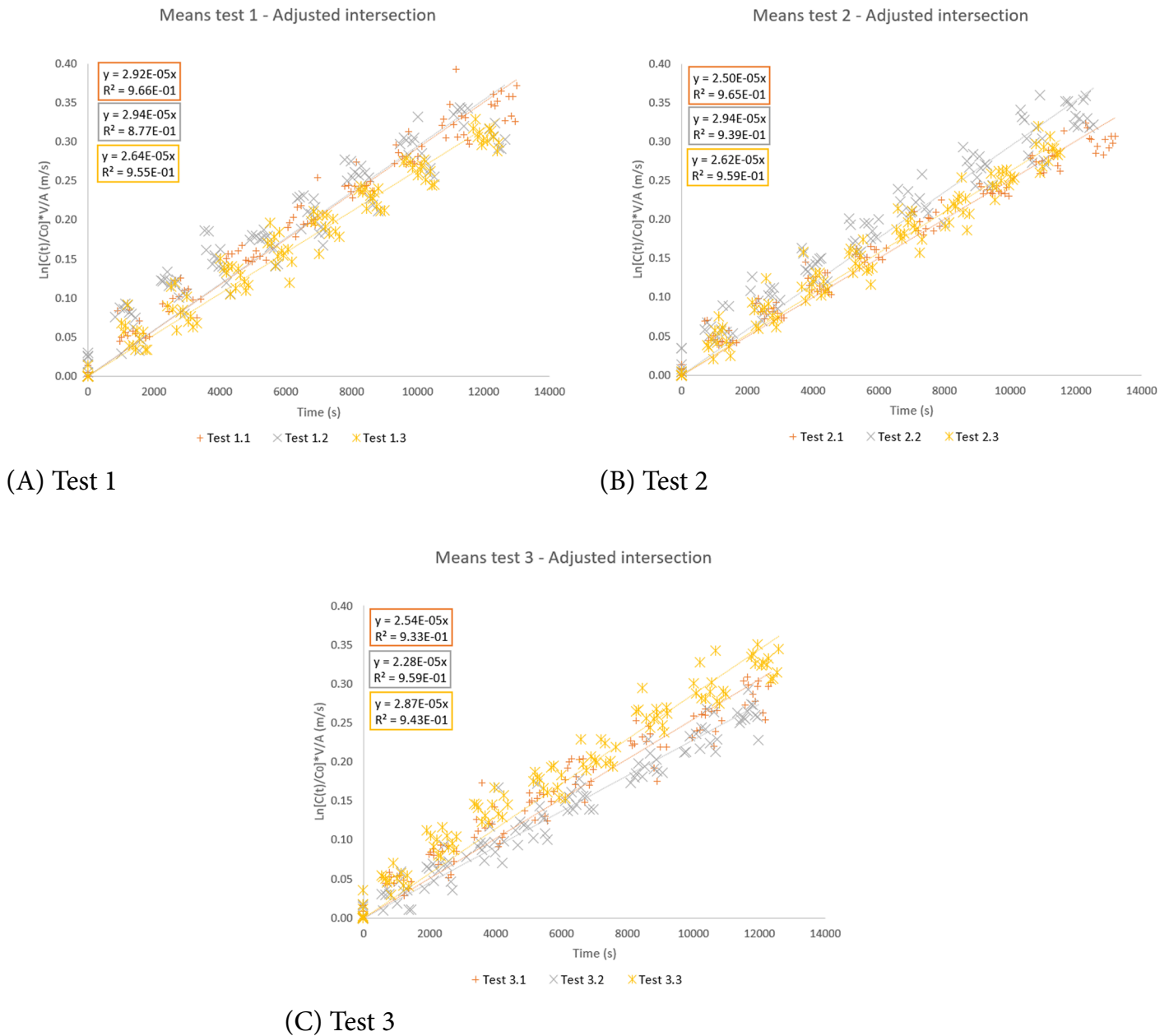

(A) Test 1

(B) Test 2

(C) Test 3

Figure 3 – Linear adjustment to the mean of all points to obtain the global mass transfer coefficient with forced intersection.
y: fitting equation; R^2: coefficient of determination.

Values of the R^2 were lower for the cases in which the intersection was adjusted to the origin, but they were still high.

Analysis of the variation in the global mass transfer coefficient between each flow rate and each sampling point

In test 1, the coefficient of variation is between 4.7 and 11.3%, with the highest value at point 5. In test 2, however, despite the low coefficient of variation at point 6, there is a general increase in variability, with coefficients varying between 4.7 and 11.4%, with the highest value at point 4. The highest coefficients of variation are observed in test 3, where they are between 8.5 and 16.0%, with the highest value at point 1 (Tables 1, 2 and 3).

Table 1 – Values of global mass transfer coefficient (m s⁻¹) for hydrogen sulfide. Test 1 with forced intersection at the origin.

Point	Test 1.1	Test 1.2	Test 1.3	Mean	SD	CV
1	3.04E-05	3.33E-05	2.95E-05	3.11E-05	1.99E-06	6.4%
2	2.82E-05	2.99E-05	2.68E-05	2.83E-05	1.55E-06	5.5%
3	2.96E-05	3.22E-05	2.82E-05	3.00E-05	2.03E-06	6.8%
4	2.81E-05	2.68E-05	2.56E-05	2.68E-05	1.25E-06	4.7%
5	3.16E-05	3.13E-05	2.57E-05	2.95E-05	3.32E-06	113.0%
6	2.76E-05	2.46E-05	2.33E-05	2.52E-05	2.21E-06	8.8%

SD: standard deviation; CV: coefficient of variation.

Table 2 – Values of global mass transfer coefficient (m s⁻¹) for hydrogen sulfide. Test 2 with forced intersection at the origin.

Point	Test 2.1	Test 2.2	Test 2.3	Mean	SD	CV
1	2.75E-05	3.30E-05	2.83E-05	2.96E-05	2.97E-06	10.0%
2	2.49E-05	2.99E-05	2.81E-05	2.76E-05	2.53E-06	9.2%
3	2.54E-05	3.04E-05	2.50E-05	2.69E-05	3.01E-06	11.2%
4	2.43E-05	3.00E-05	2.54E-05	2.66E-05	3.02E-06	11.4%
5	2.41E-05	2.77E-05	2.67E-05	2.62E-05	1.86E-06	7.1%
6	2.44E-05	2.61E-05	2.39E-05	2.48E-05	1.15E-06	4.7%

SD: standard deviation; CV: coefficient of variation.

Table 3 – Values of global mass transfer coefficient (m s⁻¹) for hydrogen sulfide. Test 3 with forced intersection at the origin.

Point	Test 3.1	Test 3.2	Test 3.3	Mean	SD	CV
1	2.66E-05	2.24E-05	3.09E-05	2.66E-05	4.25E-06	16.0%
2	2.70E-05	2.54E-05	3.00E-05	2.75E-05	2.34E-06	8.5%
3	2.74E-05	2.35E-05	3.04E-05	2.71E-05	3.46E-06	12.8%
4	2.16E-05	2.32E-05	2.62E-05	2.37E-05	2.34E-06	9.9%
5	2.47E-05	2.02E-05	2.74E-05	2.41E-05	3.64E-06	15.1%
6	2.58E-05	2.23E-05	2.80E-05	2.54E-05	2.87E-06	11.3%

SD: standard deviation; CV: coefficient of variation.

An initial analysis showed that the points located just after the expansion section had higher average K_L values. This behavior can be explained by the jet effect caused by the curvature of the development pipe, as explained by Siqueira (2022), which accelerates the flow generating a slight disturbance at the beginning of the section, but does not form a wave on any scale. Despite this substantial increase at the start of the test section, the standard deviation of the measurement at each point should be analyzed to check whether the values are within the same range or whether the values are actually higher in this region.

Figure 4 shows the average values of the K_L for each point in each test conducted. In Figure 4A, all the mean values obtained at each point in test 1 are higher than those in test 2. The values for test 2, except for points 3 and 6, are higher than those for test 3. In addition, in tests 1 and 2, points 1, 3, and 5, on the right side of the tunnel in the direction of the flow, have higher average K_L values than points 2, 4, and 6 on the left side of the PWT, which indicates a possible asymmetry in the mass transfer inside the tunnel.Despite the trends observed, it can be seen that the standard deviation, represented by the lines in the upper region of the bars, does not differ from test to test and consequently all the points can be represented by a mean value of the three tests at the same point. Thus, Figure 5 shows the mean values between all the tests for each point measured, in which it is observed that the average K_L values of the odd-numbered points (right side of the tunnel) are slightly higher than the even-numbered points (left side of the device). To verify this hypothesis, we applied the one-tailed F-test with a 95% confidence interval. This hypothesis was confirmed only for test 1 ($p<0.05$), but was invalid for the other two tests. In summary, despite the general trend, the difference in K_L mean values between odd and even points was only statistically significant for the first test. This suggests that, under specific conditions, there may be a slight asymmetry in mass transfer within the wind tunnel, but this difference does not remain consistent in all the tests conducted.

It should also be noted that although mean values are different from each other, the standard deviations for the measurements taken, represented by the error bars in Figure 5, show a range that covers all the points. Thus, it is understood that there was no spatial variation in the K_L, in which K_L can be considered the same over the liquid surface for the experiments conducted.

Consequently, knowing that the mass transfer values did not vary spatially and among the flow rates studied, Figure 6 shows the concentration decay curve for all the tests, which shows $R^2=0.935$. Therefore, by linearly adjusting the equation in logarithmic form for all the tests and forcing the adjustment to the origin, the K_L value of H_2S is obtained for the PWT for measuring odorous compounds, in which $K_L=2.70 \times 10^{-5} \pm 2.99 \times 10^{-6}$ m s⁻¹.

Comparison between experimental global mass transfer coefficient and that estimated by empirical models

Empirical models aim to determine the K_L for the liquid and gas phases, respectively K_L and K_G, in order to obtain the K_L, by fitting curves obtained from experimental methods.

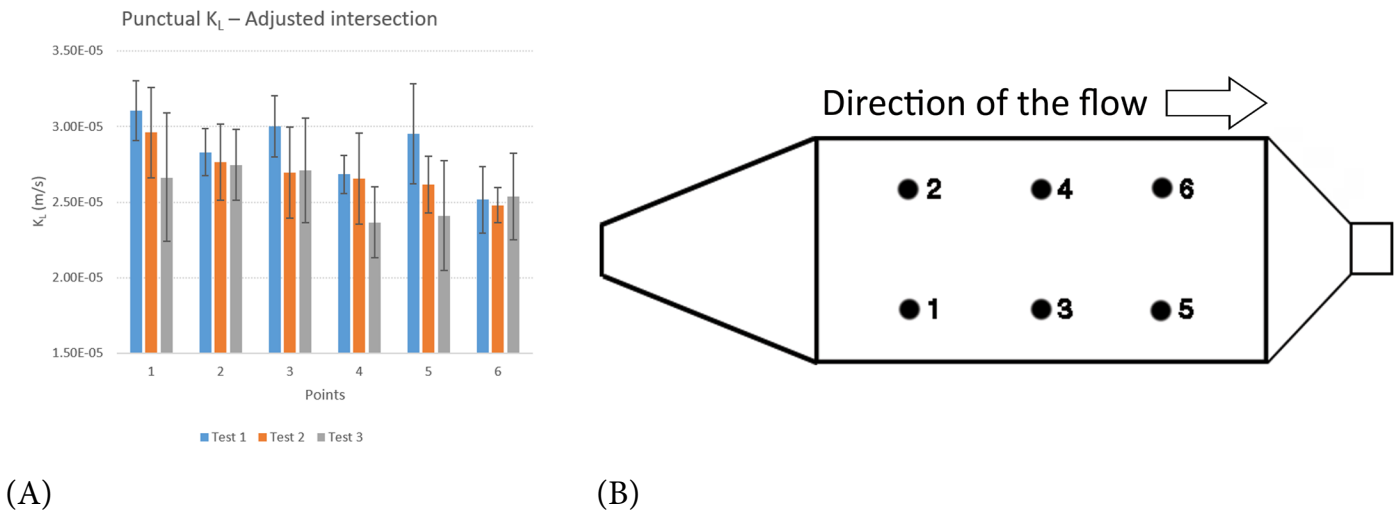(A)   (B)

Figure 4 – Mean of the global mass transfer coefficient values (A) for each point with the adjustment at the intersection for the wind tunnel sampling points (B).
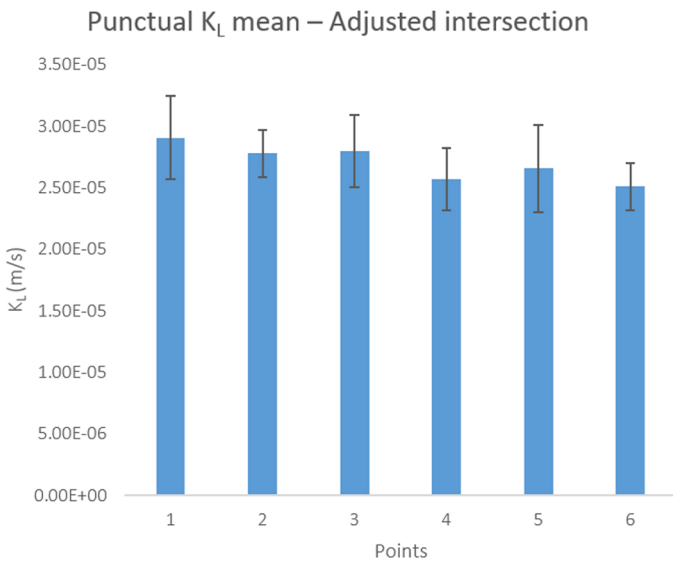

Figure 5 – Global mass transfer coefficient values with the mean of all the tests for each point.

However, these models were developed for application in real cases, i.e., ponds with certain dimensions and wind speeds consistent with reality. Therefore, in this work, the comparison of the obtained K_L with the mass coefficients determined using dimensions and flow conditions within the empirical models was conducted to differentiate, in order of magnitude, what was measured in the PWT compared to analogous situations in the field.

Thus, in order to understand the behavior of the wind tunnel, empirical models were applied with parameters similar to those used in the laboratory experiment. However, as the friction velocity was not

estimated in the experiments, this parameter was based on Siqueira (2022), who conducted numerical simulations with PWTs of the same geometry, dimensions, and flow conditions, in which the contact surface was considered a flat plate. The experimental K_L values and K_L values from the main models in the literature are shown in Table 4.

Gostelow et al. (2001) showed the greatest proximity to the values found experimentally in tests 2 and 3, with all coefficients being in the same order of magnitude. After Gostelow et al. (2001), the model that presented coefficients closest to those measured in the laboratory were found by US EPA (1994). For the tunnel conditions applied to this model, mass transfer was dominated only by diffusion, which justifies the close values for the various flow rates, but the K_L values were around 5 to 6-times higher than the coefficients obtained in the experiments.

Prata et al. (2018b) showed lower values for lower flow rates, which is expected, due to the proportionality of the friction speed. However, the K_L obtained in the laboratory for H_2S were between 5.8 (test 3.2) and 16.4 (test 1.1) times higher than the K_L obtained by the empirical model. Mackay and Yeun (1983) presented the model with the greatest variation in K_L, in which experimental values were between 4.8 and 17.5 times greater than those calculated by the model.

The numerical discrepancies in K_L values between the empirical models and the experiment can be explained by a number of factors, such as differences in the uncontrolled variables (temperature, humidity, and atmospheric pressure), the scale of experiments, and the geometry of the apparatus. These differences can affect the flow and, consequently, not accurately simulate the real conditions in which the mass transfer phenomenon occurs. This phenomenon, in turn, is extremely complex and dependent on local conditions, many of which are simplified by models to make them more controllable, while practi-
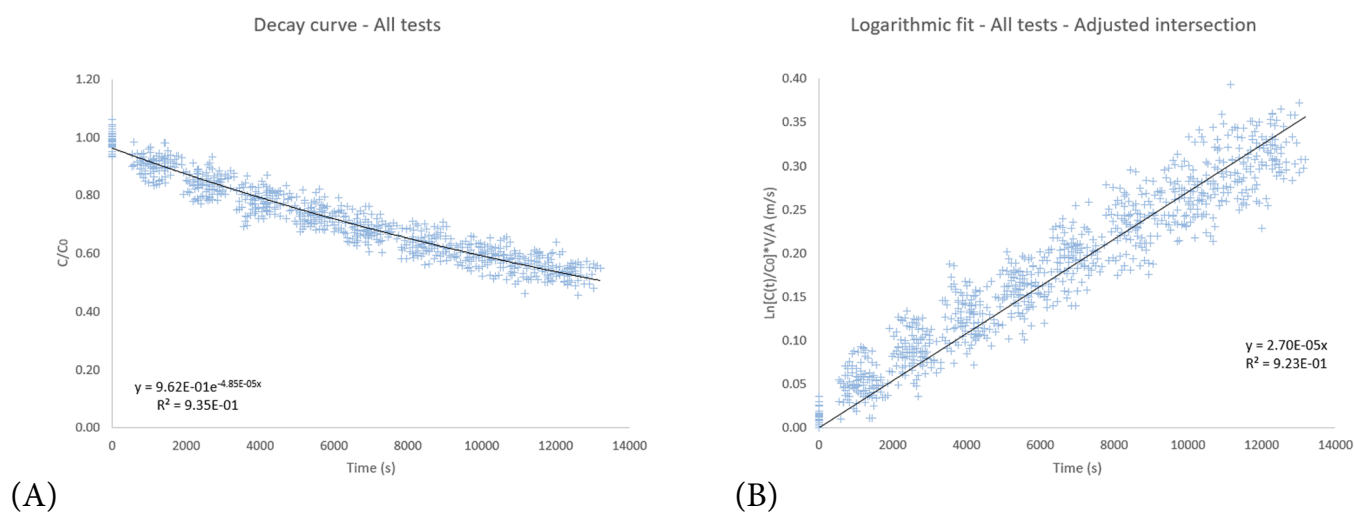
(A)

(B)

Figure 6 – Adjustments considering all the tests to evaluate (A) concentration decay with exponential adjustment and (B) the obtention of the global mass transfer coefficient with linear adjustment and forced intersection at the origin, applied to the equation in logarithmic form.

Table 4 – Values of the global mass transfer coefficients (m s⁻¹) experimentally obtained and calculated using empirical models.

Test	This work	Mackay and Yeun (1983)	Gostelow et al. (2001)	Prata et al. (2018b)	US EPA (1994)
1	2.59E-05	1.55E-06	6.03E-06	1.63E-06	4.40E-06
2	2.48E-05	2.95E-06	1.07E-05	2.89E-06	4.40E-06
3	2.36E-05	4.54E-06	1.41E-05	3.79E-06	4.40E-06

cal experiments can provide more detail. Thus, it is essential to realize and study the limitations and potential of both methods for a more accurate estimate of the coefficients discussed in this work.

The K_L values obtained in test 3 ($u_*=0.097$ m s⁻¹) were compared to the experimental data presented by Santos et al. (2012) with friction speed values of 0.11 m s⁻¹, which gave values of K_L equal to 1.28, 2.79, and 2.18 (x 10⁻⁶ m s⁻¹). Comparing these values with those obtained in this study, it can be seen that they were 7.8 to 18.0 times higher than those obtained by Santos et al. (2012). Thus, for the conditions studied, it can be inferred that the PWT overestimated the values of the K_L compared to the main empirical models in the literature.

Conclusions

This study conducted PWT experiments aimed at analyzing the mass transfer of H_2S emitted from a liquid surface. Samples were col-

lected at six different points in the apparatus. The technique used to analyze the decay of the liquid phase was spectrophotometry and, using these values, the K_L were calculated for each point.

Analysis of the average K_L values indicated there was no significant spatial variation in the K_L along the PWT. Thus, the mean K_L value found for H_2S was 2.7×10^{-5} m s⁻¹.

The experimental K_L values were compared to the main empirical models in the literature. The model by Gostelow et al. (2011) was the one with numerical values closest to those obtained in the experiment. It should be noted that numerical differences between the experimental and empirical methods are due to several reasons, including experimental conditions and simplifications employed by the models.

This study has made it possible to understand the H_2S mass transfer process inside the PWT and has broadened our knowledge of the behavior of this device. Further experimental work on mass transfer should therefore be conducted in order to verify the effectiveness of emission estimate with the PWT under practical conditions. In addition, numerical studies can be used considering the K_L values found in order to observe the influence of geometry on the emission inside the PWT. Advances in the study of the method to quantify odor emissions may enable standards to be drawn up for the control of this pollutant and will facilitate the monitoring of such emissions in sanitation companies.

References

Andreão, W.L.; Santos, J.M.; Reis, N.C.; Prata, A.A.; Stuetz, R.M., 2019. Effects of flux chamber configuration on the sampling of odorous gases emissions. International Journal of Heat and Mass Transfer, v. 140, 918-930. https://doi.org/10.1016/j.ijheatmasstransfer.2019.06.029

Arogo, J.; Zhang, R.H.; Riskowski, G.L.; Day, D.L., 1999. Mass transfer coefficient for hydrogen sulfide emission from aqueous solutions and liquid swine manure. Transactions of the ASAE, v. 42, (5), 1455-1462. https://doi.org/10.13031/2013.13309

Capelli, L.; Sironi, S.; Del Rosso, R.; Guillot, J.-M., 2013. Measuring odours in the environment vs.Dispersion modelling: a review.pdf. Atmospheric Enviroment, v. 79, 731-743. https://doi.org/10.1016/j.atmosenv.2013.07.029

Deacon, E.L., 1977. Gas transfer to and across an air-water interface. Tellus, v. 29, (4), 363-374. https://doi.org/10.1111/j.2153-3490.1977.tb00746.x

Gostelow, P.; Parsons, S.A.; Cobb, J., 2001. Development of an adorant emission model for sewage treatment works. Water Science and Technology, v. 44, (9), 181-188. https://doi.org/10.2166/wst.2001.0535.

Guillot, J.M.; Clincke, A.S.; Guilleman, M., 2014. Odour emission from liquid and solid area sources: A large intercomparison of sampling devices. Chemical Engineering Transactions, v. 40, (Special Issue), 151-156. https://doi.org/10.3303/CET1440026

Hudson, N.; Ayoko, G.A., 2008a. Odour sampling. 2. Comparison of physical and aerodynamic characteristics of sampling devices: A review. Bioresource Technology, v. 99, (10), 3993-4007. https://doi.org/10.1016/j.biortech.2007.03.043

Hudson, N.; Ayoko, G.A., 2008b. Odour sampling 1: Physical chemistry considerations. Bioresource Technology, v. 99, (10), 3982-3992. https://doi.org/10.1016/j.biortech.2007.04.034

Jiang, K.; Bliss, P.J.; Schulz, T.J., 1995. The development of a sampling system for determining odor emission rates from areal surfaces: Part i. aerodynamic performance. Journal of the Air and Waste Management Association, v. 45, (11), 917-922. https://doi.org/10.1080/10473289.1995.10467424

Jiang, G.; Melder, D.; Keller, J.; Yuan, Z., 2017. Odor emissions from domestic wastewater: a review. Critical Reviews in Environmental Science and Technology, v. 47, (17), 1581-1611. https://doi.org/10.1080/10643389.2017.1386952

Liu, L.; Abdala Prata Junior, A.; Fisher, R.M.; Stuetz, R.M., 2022. Measuring volatile emissions from biosolids: A critical review on sampling methods. Journal of Environmental Management, v. 317, 115290. https://doi.org/10.1016/j.jenvman.2022.115290

Liu, Y.; Lu, W.; Li, D.; Guo, H.; Caicedo, L.; Wang, C.; Xu, S.; Wang, H., 2015. Estimation of volatile compounds emission rates from the working face of a large anaerobic landfill in China using a wind tunnel system. Atmospheric Environment, v. 111, 213-221. https://doi.org/10.1016/j.atmosenv.2015.04.017

Lucernoni, F.; Capelli, L.; Busini, V.; Sironi, S., 2017. A model to relate wind tunnel measurements to open field odorant emissions from liquid area sources. Atmospheric Environment, v. 157, 10-17. https://doi.org/10.1016/j.atmosenv.2017.03.004

Mackay, D.; Yeun, A.T.K., 1983. Mass transfer coefficient correlations for volatilization of organic solutes from water. Environmental Science and Technology, v. 17, (4), 211-217. https://doi.org/10.1021/es00110a006

Pouly, F.; Touraud, E.; Buisson, J.F.; Thomas, O., 1999. An alternative method for the measurement of mineral sulphide in wastewater. Talanta, v. 50, (4), 737-742. https://doi.org/10.1016/S0039-9140(99)00201-5

Prata, A.A.; Lucernoni, F.; Santos, J.M.; Capelli, L.; Sironi, S.; Le-Minh, N.; Stuetz, R.M., 2018a. Mass transfer inside a flux hood for the sampling of gaseous emissions from liquid surfaces – Experimental assessment and emission rate rescaling. Atmospheric Environment, v. 179, 227-238. https://doi.org/10.1016/j.atmosenv.2018.02.029

Prata, A.A.; Santos, J.M.; Beghi, S.P.; Fernandes, I.F.; Vom Marttens, L.L.C.; Pereira Neto, L.I.; Martins, R.S.; Reis, N.C.; Stuetz, R.M., 2016. Dynamic flux chamber measurements of hydrogen sulfide emission rate from a quiescent surface - A computational evaluation. Chemosphere, v. 146, 426-434. https://doi.org/10.1016/j.chemosphere.2015.11.123

Prata, A.A.; Santos, J.M.; Timchenko, V.; Stuetz, R.M., 2018b. A critical review on liquid-gas mass transfer models for estimating gaseous emissions from passive liquid surfaces in wastewater treatment plants. Water Research, v. 130, 388-406. https://doi.org/10.1016/j.watres.2017.12.001

Prata, A.A.; Santos, J.M.; Timchenko, V.; Stuetz, R.M., 2014. Use of Computational Fluid dynamics in the analysis of a portable wind tunnel for sampling of odorous emissions at liquid surfaces. Chemical Engineering Transactions, v. 40, (Special Issue), 145-150. https://doi.org/10.3303/CET1440025

Santos, J.M.; Kreim, V.; Guillot, J.M.; Reis, N.C.; De Sá, L.M.; Horan, N.J., 2012. An experimental determination of the H 2S overall mass transfer coefficient from quiescent surfaces at wastewater treatment plants. Atmospheric Environment, v. 60, 18-24. https://doi.org/10.1016/j.atmosenv.2012.06.014

Siqueira, M.A., 2022. Influence of the design and operational conditions on the airflow and mass transfer phenomena inside a portable wind tunnel used to estimate odorant compounds measured over passive liquid surfaces. Master Thesis, Universidade Federal do Espírito Santo, Espírito Santo.

Suffet, I.; Braithwaite, S., 2019. White Paper: Odor Complaints, Health Impacts and Monitoring Methods. University of California, (18), 176-200 (Accessed November 10, 2023) at:. https://ww2.arb.ca.gov/sites/default/files/classic/research/apr/past/18rd010.pdf.

Teixeira, S.A.; Pereira, P.D.; Ferreira, F.C., 2018. Atmospheric odours: Monitoring of an urban waste operator with citizen participation. Chemical Engineering Transactions, v. 68, 91-96. https://doi.org/10.3303/CET1868016

Tran, H.N.Q.; Lyman, S.N.; Mansfield, M.L.; O'Neil, T.; Bowers, R.L.; Smith, A.P.; Keslar, C., 2018. Emissions of organic compounds from produced water ponds II: Evaluation of flux chamber measurements with inverse-modeling techniques. Journal of the Air and Waste Management Association, v. 68, (7), 713-724. https://doi.org/10.1080/10962247.2018.1426654

United States Environmental Protection Agency (US EPA), 1994. Air Emissions Models for Waste and Wastewater. US Environmental Protection Agency, EPA-453/R-94-080A. Research Triangle Park, North Carolina (Accessed November 10, 2023) at:. https://www3.epa.gov/ttnchie1/software/water/air_emission_models_waste_wastewater.pdf

Vitko, T.G.; Cowden, S.; Suffet, I.H., 2022a. Mel. Evaluation of bioscrubber and biofilter technologies treating wastewater foul air by a new approach of using odor character, odor intensity, and chemical analyses. Water Research, v. 220, 118691. https://doi.org/10.1016/j.watres.2022.118691

Wang, X.; Jiang, J.; Kaye, R., 2001. Improvement of a wind-tunnel sampling system for odour and VOCs. Water Science and Technology, v. 44, (9), 71-77. https://doi.org/10.2166/wst.2001.0511